Eur. Phys. J. Special Topics **160**, 331–342 (2008)

DOI: 10.1140/epjst/e2008-00736-5

THE EUROPEAN PHYSICAL JOURNAL SPECIAL TOPICS

From squeezed atom lasers to teleportation of massive articles

M.K. Olsen[1,a], S.A. Haine[1], A.S. Bradley[1], and J.J. Hope[2]

[1] ARC Centre of Excellence for Quantum-Atom Optics, School of Physical Sciences, University of Queensland, Queensland 4072, Australia
[2] ARC Centre of Excellence for Quantum-Atom Optics, Department of Physics, Australian National University, Canberra, ACT, Australia

Abstract. The development of the Raman atom laser promises to make available new techniques for accessing and manipulating the quantum statistical properties of Bose-Einstein condensates. In this work we show how, combined with the already existing methods for the manipulation of quantum states of light which are central to quantum optics, the Raman input-output coupling mechanisms potentially enable the production of quadrature squeezed and sub-Poissonian atomic beams, and entanglement between atomic and optical fields. We also propose a method of measuring the quantum statistics of the atomic beam by transferring them to an optical field. Finally, by combning these techniques, we propose a method of teleporting the atom laser beam from one trapped condensate to another.

1 Introduction

Quantum-atom optics [1–3] is a rapidly developing subfield of ultra-cold atomic physics. The development of the Raman output coupler [4], which can produce controlled and potentially coherent atomic beams, will make available new techniques and phenomena in quantum-atom optics, just as the optical laser did in quantum optics. One interesting possibility is the production of atomic beams in states analogous to the squeezed and entangled states of the optical field which are now routinely produced in laboratories [5]. In this work we will cover proposed methods for producing nonclassical matter wave states and measuring the quantum properties of these using the ability of Raman output and input coupler mechanisms to transfer quantum statistics between atomic and optical fields. Beginning with the production of sub-Poissonian atomic beams [6], including the entanglement of atomic and optical fields [7] and the transfer of statistics to an optical field to allow for simple homodyne measurements [8,9], we will finally demonstrate how the input [10] and output couplers can be combined to teleport an atomic beam from one location to another without the need for sharing of entanglement resources [11].

Previously proposed methods for producing matter waves in highly non-classical states include utilising the nonlinear atomic interactions to create correlated pairs of atoms via either molecular down conversion [12], spin exchange collisions [13,14], or by transferring the quantum state of a non-classical electromagnetic field to a propagating atomic field [15–17]. In some of these schemes it has been demonstrated that continuous variable entanglement can be generated between spatially separated atomic beams [12,15] or between an atomic beam and an optical beam [7]. Here we show how the flexibility of our system can be used to do many of these with the one basic experimental setup.

[a] e-mail: mko@physics.uq.edu.au

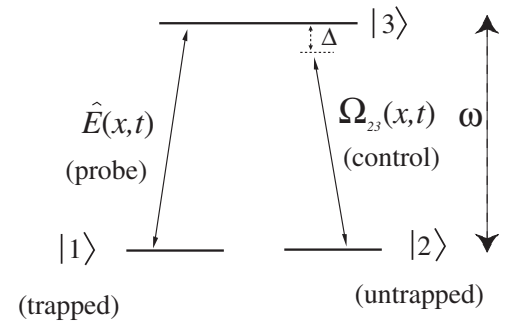

Fig. 1. Internal energy levels of our three-level atom. A condensate of state $|1\rangle$ atoms is coupled to an untrapped state via a Raman transition. The two fields of the Raman transition are a probe beam (annihilation operator $\hat{E}(x,t)$) and a control field, which is strong compared to the probe beam and can be approximated by a classical field ($\Omega_{23}(x,t)$), detuned from the excited state by an amount Δ.

2 Theoretical model of a Raman atom laser

In this work we are interested in the transfer of quantum states between atom laser beams and optical fields. We begin here by outlining our approach to the basic atom-light interaction which is central to all subsequent sections. We model the system as a one-dimensional BEC of three-level atoms outcoupled via a Raman transition, as in Fig. 1. The BEC is confined in a magnetic trap and manipulated by two laser fields. A photon from the probe beam is absorbed, and one is emitted into the control beam, transferring the internal state of the atom from $|1\rangle$ (trapped) to $|2\rangle$ (untrapped) and giving the atom a momentum kick of $\hbar(\mathbf{k}_{\text{probe}} - \mathbf{k}_{\text{control}})$, forming an atom laser beam.

The Hamiltonian for the system is

$$\begin{aligned}\mathcal{H} &= \mathcal{H}_{\text{atom}} + \mathcal{H}_{\text{int}} + \mathcal{H}_{\text{light}} \qquad (1)\\ &= \int \hat{\psi}_1^\dagger(x) H_0 \hat{\psi}_1(x) dx + \int \hat{\psi}_2^\dagger(x) \left(-\frac{\hbar^2}{2m}\nabla^2\right) \hat{\psi}_2(x) dx + \int \hat{\psi}_3^\dagger(x) \left(-\frac{\hbar^2}{2m}\nabla^2 + \hbar\omega_0\right) \hat{\psi}_3(x) dx\\ &+ \hbar \int (\hat{\psi}_2(x)\hat{\psi}_3^\dagger(x)\Omega_{23}(x,t) + h.c.)\, dx + \hbar g_{13} \int (\hat{E}(x)\hat{\psi}_1(x)\hat{\psi}_3^\dagger + h.c.)\, dx + \mathcal{H}_{\text{light}}\end{aligned}$$

where $\Omega_{23}(x,t) = \Omega_{23} e^{i(k_0 x - (\omega_0 - \Delta)t)}$ is the Rabi frequency for the $|2\rangle \rightarrow |3\rangle$ transition, H_0 is the single particle Hamiltonian for the trapped atoms, m is the atomic mass, $\hat{\psi}_1(x)$ is the annihilation operator for the condensate mode (internal state $|1\rangle$), $\hat{\psi}_3(x)$ is the annihilation operator for the excited atoms ($|3\rangle$), and $\hat{\psi}_2(x)$ is the annihilation operator for the untrapped atoms ($|2\rangle$). The atomic field operators obey bosonic commutation relations,

$$[\hat{\psi}_i(x), \hat{\psi}_j(x')] = [\hat{\psi}_i^\dagger(x), \hat{\psi}_j^\dagger(x')] = 0, \qquad (2)$$

and

$$[\hat{\psi}_i(x), \hat{\psi}_j^\dagger(x')] = \delta_{ij}\delta(x - x'). \qquad (3)$$

$\hat{E}(x)$ is the spatially dependent annihilation operator for the probe field, satisfying $[\hat{E}(x), \hat{E}^\dagger(x')] = \delta(x - x')$. The coupling coefficient is $g_{13} = \frac{d_{13}}{\hbar}\sqrt{\frac{\hbar\omega_k}{2\epsilon_0 A}}$, where d_{13} is the dipole moment for the $|1\rangle \rightarrow |3\rangle$ transition, and A is the cross sectional area of the beam. We assume that $g_{13}(\omega_k)$ is approximately flat in the interaction region range. In one dimension,

$$\mathcal{H}_{\text{light}} = -ic\hbar \int \hat{E}^\dagger(x) \frac{\partial}{\partial x} \hat{E}(x)\, dx. \qquad (4)$$

The equations of motion for the Heisenberg operators are found as

$$\begin{aligned}
i\dot{\hat{\psi}}_1(x) &= \frac{H_0}{\hbar}\hat{\psi}_1(x) + g_{13}\tilde{\psi}_3(x)\tilde{E}^\dagger(x),\\
i\dot{\hat{\psi}}_2(x) &= -\frac{\hbar}{2m}\nabla^2\hat{\psi}_2(x) + \Omega_{23}^* e^{-ik_0x}\hat{\psi}_3(x),\\
i\dot{\tilde{\psi}}_3(x) &= \left(-\frac{\hbar}{2m}\nabla^2 + \Delta\right)\tilde{\psi}_3(x) + \Omega_{23}e^{ik_0x}\hat{\psi}_2(x) + g_{13}\tilde{E}(x)\hat{\psi}_1(x),\\
i\dot{\tilde{E}}(x) &= \left(-ic\frac{\partial}{\partial x} - (\omega_0 - \Delta)\right)\tilde{E}(x) + g_{13}\hat{\psi}_1(x)\tilde{\psi}_3^\dagger(x),
\end{aligned} \tag{5}$$

where $\tilde{\psi}_3(x) = \hat{\psi}_3 \mathrm{e}^{i(\omega_0-\Delta)t}$ and $\tilde{E}(x) = \hat{E}\mathrm{e}^{i(\omega_0-\Delta)t}$. The population of the excited state $|3\rangle$ will be insignificant when the detunings of the optical fields are larger than the other terms in the system and, since the dynamics occur on time scales greater than $\frac{1}{\Delta}$, we can set $\tilde{\psi}_3(x) = -\frac{\Omega_{23}}{\Delta}\mathrm{e}^{ik_0x}\hat{\psi}_2(x) - \frac{g_{13}}{\Delta}\tilde{E}(x)\hat{\psi}_1$. Using this approximation, the equations of motion for the probe field and the atom laser beam become

$$i\dot{\hat{\psi}} = H_2\hat{\psi}(x) - \Omega_c\tilde{E}(x) \tag{6}$$

$$i\dot{\tilde{E}}(x) = H_E\tilde{E}(x) - \Omega_c^*\hat{\psi}(x) \tag{7}$$

with $\tilde{E} \equiv \hat{E}(x)\mathrm{e}^{i(\omega_0-\Delta)t)}$, $\hat{\psi}(x) \equiv \hat{\psi}_2(x)$, $\Omega_c = \frac{g_{13}\Omega_{23}^*}{\Delta}\mathrm{e}^{-ik_0x}\phi_1(x)$ and $H_2 = -\frac{\hbar}{2m}\nabla^2 - \frac{|\Omega_{23}|^2}{\Delta}$, and $H_E = -ic\frac{\partial}{\partial x} - (\omega_0 - \Delta) - \frac{|g_{13}|^2}{\Delta}|\phi_1(x)|^2$, with $\phi_1(x,t) \equiv \langle\hat{\psi}_1(x)\rangle$ representing the semiclassical wavefunction for the condensate atoms. We consider that the trapped condensate remains in a coherent state i.e. $\hat{\psi}_1(x) \approx \langle\hat{\psi}_1(x)\rangle \equiv \phi_1(x)$, which is valid if the number of atoms outcoupled is small compared to the total number. We have assumed that the condensate is dilute enough that collisional interactions can be ignored. (The interactions could also be tuned by Feshbach resonance techniques [18].) The evolution of the condensate mode is then given by

$$i\dot{\phi}_1(x) = \left(\frac{H_0}{\hbar} - \frac{g_{13}^2}{\Delta}\langle\tilde{E}^\dagger(x)\tilde{E}(x)\rangle\right)\phi_1(x) - \Omega_c\langle\hat{E}^\dagger(x)\hat{\psi}(x)\rangle. \tag{8}$$

We note here that we are using a one dimensional analysis for three reasons. The first is that the interesting dynamics takes place along one direction. The second is that it is experimentally possible to realise an effective one dimensional system by, for example, confinement in a waveguide. The third is that it would be extremely difficult to use our calculational method in more than one dimension.

In order to solve Eqs. (6) and (7), we expand the field operators at $t = 0$ as

$$\hat{\psi}(x, t=0) = \sum_i f_i(x)\hat{a}_i \qquad \text{and} \qquad \tilde{E}(x, t=0) = \sum_i p_i(x)\hat{b}_i, \tag{9}$$

where $f_i(x)$ and $p_i(x)$ represent an expansion in any orthonormal basis, and the operators $\hat{a}_i$ and $\hat{b}_i$ represent Schrödinger picture operators for the ith mode of the atomic and optical fields respectively. We can now postulate solutions to Eq. (6) and (7) as

$$\hat{\psi}(x,t) = \sum_i f_i(x,t)\hat{a}_i + \sum_i g_i(x,t)\hat{b}_i \tag{10}$$

$$\tilde{E}(x,t) = \sum_i p_i(x,t)\hat{b}_i + \sum_i q_i(x,t)\hat{a}_i. \tag{11}$$

By substituting this ansatz into Eqs. (6) and (7) we obtain equations of motion for the mode functions $f_i(x)$, $g_i(x)$, $p_i(x)$ and $q_i(x)$, given by

$$i\dot{f}_i(x) = H_2 f_i(x) - \Omega_c q_i(x) \tag{12}$$

$$i\dot{g}_i(x) = H_2 g_i(x) - \Omega_c p_i(x) \tag{13}$$

$$i\dot{p}_i(x) = H_E p_i(x) - \Omega_c^* g_i(x) \tag{14}$$

$$i\dot{q}_i(x) = H_E q_i(x) - \Omega_c^* f_i(x) \tag{15}$$

with $g_i(x, t = 0) = q_i(x, t = 0) = 0$. In practice we may choose any initial conditions for the $f_i(x)$s and $p_i(x)$s, as long as they form an orthonormal basis. The solutions to these equations make available the dynamics of any system observable. Another simplification is that in our system we initially have no outcoupled atoms, and can choose a basis so that the photons initially occupy only one mode. i.e. $|\Psi(t = 0)\rangle = |0, 0, \ldots, 0\rangle_{atoms} \otimes |\gamma, 0, \ldots, 0\rangle_{\text{light}}$, where $|\gamma\rangle$ represents an arbitrary state of a single optical mode. In subsequent calculations we choose the mode basis as plane waves, with $\hat{b}_0$ representing the annihilation operator for a plane wave with momentum $\mathbf{k}_p$, meaning that $p_0(x)$ is initially a plane wave with momentum $\mathbf{k}_p$.

Noticing that $\hat{a}_i$, for all i and $\hat{b}_i$, $(i \neq 0)$ acting on our state return zero for all time, we can find the expectation value of any normally ordered operator by making the substitution $\hat{\psi}(x) \to g_0(x)\hat{b}_0$, $\hat{E}(x) \to p_0(x)\hat{b}_0$. This is only true when the operators are in normally ordered form before the substitution is made. In terms of Eqs. (10) and (11), Eq. (8) can be written as

$$i\dot{\phi}_1(x) = \left(\frac{H_0}{\hbar} - \frac{|g_{13}|^2}{\Delta}\langle\hat{b}_0^\dagger\hat{b}_0\rangle|\bar{p}_0(x)|^2\right)\phi_1(x) - \Omega_c(x)\langle\hat{b}_0^\dagger\hat{b}_0^\dagger\rangle\bar{p}_0^*(x)\bar{g}_0(x)\,. \tag{16}$$

The equation of motion for $p_0(x)$ is difficult to solve in practice due to the high propagation speed of light. If we look more closely at the equation of motion for $p_0(x)$ (making the transformation $\tilde{p}_0(x) = p_0(x)\mathrm{e}^{i\delta t}$, $\tilde{g}_0(x) = g_0(x)\mathrm{e}^{i\delta t}$, with $\delta = c(k_c - k_p)$ the two photon detuning),

$$i\dot{\tilde{p}}_0(x) = \left(-ic\frac{\partial}{\partial x} - ck_p - \frac{|g_{13}|^2}{\Delta}|\phi_1(x)|^2\right)\tilde{p}_0(x) - \Omega_c^*(x)\tilde{g}_0(x), \tag{17}$$

we notice that $(-ic\frac{\partial}{\partial x} - \frac{|g_{13}|^2}{\Delta}|\phi_1(x)|^2)$ and ck_p are of the order of the optical frequency ($\sim 10^{15}$ Hz), but their difference is of order $c\Delta k$, where $\hbar\Delta k$ is the spread in momentum of the wave packet. Therefore the $i\dot{\tilde{p}}_0(x)$ term will be much less than the individual terms on the right hand side of Eq. (17), so that we may set the left hand side of Eq. (17) to zero if we are interested in the dynamics on time scales much longer than $\sim 1/(ck_p)$, giving

$$ic\frac{\partial\tilde{p}_0}{\partial x} = -\left(ck_p + \frac{|g_{te}|^2}{\Delta}|\phi_1(x)|^2\right)\tilde{p}_0(x) - \Omega_c^*(x)\tilde{g}_0(x). \tag{18}$$

This is a slow envelope approximation, which is valid here since the speed of light is 10 orders of magnitude faster than the mean atomic speed. In the next section, we will solve Eqs. (13), (16), and (18), and use them to investigate properties of the system.

3 A sub-Poissonian atom laser

In this section we show how a probe beam with reduced intensity fluctuations can be used to produce a sub-Poissonian atom laser. We solve Eqs. (13), (16) and (18) with typical parameters for experiments with ^{87}Rb. We set $g_{13} = (d_{13}/\hbar)\sqrt{\hbar\omega_k/2\epsilon_0 A} = 2.9 \times 10^5\,\text{rad}\,\text{s}^{-1}\,\text{m}^{\frac{1}{2}}$, where d_{13} is the dipole moment of the $|1\rangle \to |3\rangle$ transition, $\Delta = 10^{11}$ rad/s and $k_0 \equiv |\mathbf{k}_{\text{probe}} - \mathbf{k}_{\text{control}}| = 1.6 \times 10^7\,\text{m}^{-1}$. We start with a condensate of $N = 10^6$ atoms, initially in the ground state of a harmonic trap with frequency $\omega_t = 5\,\text{rad/s}$. The two photon detuning is chosen such that the coupling is on resonance, i.e. $\delta = \frac{\hbar k_0^2}{2m} - |\Omega_c|^2/\Delta - \frac{1}{2}\omega_t \equiv \delta_0$. The initial state for $p_0(x)$ is chosen as a plane wave (wave vector $|\mathbf{k}_p| = 8.0 \times 10^6\,\text{m}^{-1}$) with quantum state $|\gamma\rangle$ and a mean flux of 2.9×10^6 photons/s, with all other modes as vacuum. $p_0(x)$ is normalised on a range $\Delta x \approx 515\,\text{km}$. This defines the operator $\hat{b}_0$, with $\hat{b}_0^\dagger\hat{b}_0$ corresponding to the number of particles per Δx. A flux of 2.9×10^6 photons/s corresponds to $\langle\hat{b}_0^\dagger\hat{b}_0\rangle = 5000$.

Optimum transfer of the quantum state from the probe to the atoms occurs for unit quantum efficiency of the outcoupling. In this case the probe field is completely absorbed. In Fig. 2(a) we have chosen a value close to the optimum value of Ω_c for efficient quantum state transfer. The probe beam is almost completely absorbed, and a steady, nearly monochromatic, atomic

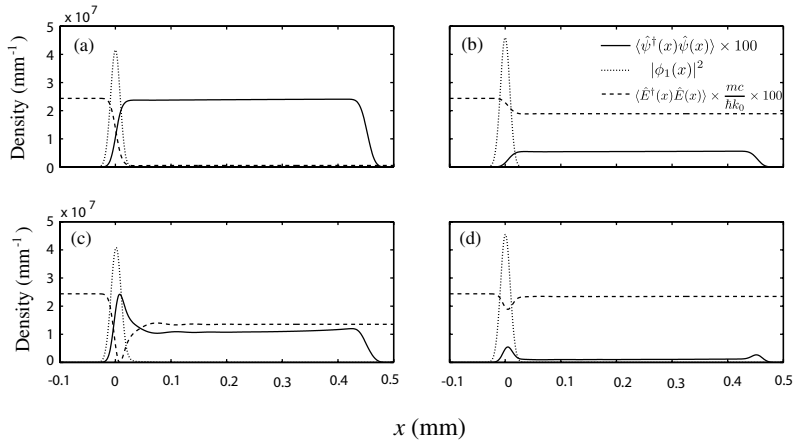

Fig. 2. Density of the condensate (dotted line), atom laser beam (solid line) and probe beam (dashed line) at $t = 40\,\mathrm{ms}$ when the system is (a) on resonance with the optimal coupling ($\Omega_c = 1.5 \times 10^8\,\mathrm{rad/s}$, $\delta = \delta_0$), (b) on resonance and under-coupled ($\Omega_c = 0.5 \times 10^8\,\mathrm{rad/s}$, $\delta = \delta_0$), (c) on resonance and over-coupled ($\Omega_c = 2.25 \times 10^8\,\mathrm{rad/s}$, $\delta = \delta_0$), and (d) off resonance with optimum coupling ($\Omega_c = 1.5 \times 10^8\,\mathrm{rad/s}$, $\delta - \delta_0 = 1500\,\mathrm{rad/s}$). The probe and control beams have been multiplied by a factor of 100 for clarity. The factor $mc/\hbar k_0 = v_{\mathrm{light}}/v_{atoms}$ is the ratio of the speed of light to the mean atomic speed. The density of the probe beam is multiplied by this ratio to show conservation of particle flux.

beam is produced. We also show an example where the system is under-coupled, with Ω_c less than the optimum. The probe beam is only partially absorbed, giving a reduced flux for the atom laser. For over coupling, where Ω_c is larger than the optimum value, we find a bound state and reduced flux. With the system at the optimum outcoupling rate, but detuned from the optimum two-photon detuning, we also see inhibited outcoupling.

The efficiency of quantum state transfer from the probe may be shown by comparing the intensity variances of the probe and the output atoms. To calculate intensity fluctuations in the atom laser, we use the density integrated over a small region. We first define the operator

$$\hat{N} = \int_{x_1}^{x_2} \hat{\psi}^\dagger(x)\hat{\psi}(x)\,dx\,, \tag{19}$$

which represents the number of atoms in a region between x_1 and x_2 in the beam path. x_1 and x_2 are chosen with $x_2 - x_1 = (\hbar k_0/mc)\Delta x$, such that when there is complete quantum state transfer, the region between x_1 and x_2 will contain exactly $\langle \hat{b}_0^\dagger \hat{b}_0 \rangle$ atoms. We now define the normalised number variance as

$$v(\hat{N}) = \frac{\langle \hat{N}^2 \rangle - \langle \hat{N} \rangle^2}{\langle \hat{N} \rangle}, \tag{20}$$

giving 0 for a Fock state and 1 for a coherent state. Figure 3 shows $v(\hat{N})$ versus time for the cases shown in Fig. 2, with the probe beam was initially in a Fock state. We see that $v(\hat{N})$ is minimised when the ideal conditions for outcoupling are met and that it slowly increases over time. This is due to the depletion of the condensate reducing the strength of the effective coupling, $\Omega(x)$. This could be compensated for by slowly increasing Ω_c or decreasing Δ. We note here that, although optical Fock states are difficult to make experimentally, their use in our analysis demonstrates that the quantum statistics are transferred efficiently between the light and the atoms.

4 Atom light entanglement

It is well known from quantum optics that it is possible to generate entanglement using one squeezed beam and vacuum incident on the two ports of a beam splitter [19]. With the effective

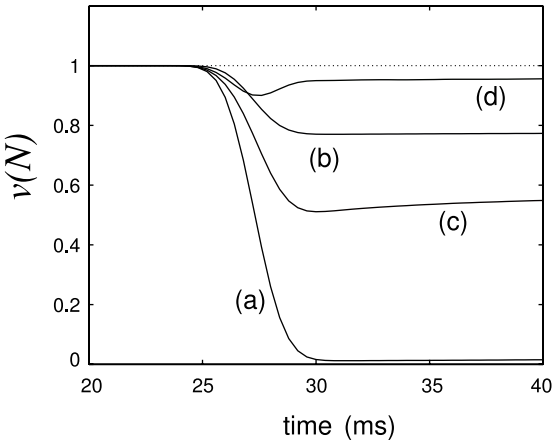

Fig. 3. $v(\hat{N})$ versus time for the cases shown in Fig. 2, with the probe initially in a Fock state. Case (a) (on resonance with optimum coupling; $\Omega_c = 1.5 \times 10^8$ rad/s, $\delta = \delta_0$), case (b) (on resonance, under-coupled; $\Omega_c = 0.5 \times 10^8$ rad/s, $\delta = \delta_0$), case (c) (on resonance, over-coupled; $\Omega_c = 2.25 \times 10^8$ rad/s, $\delta = \delta_0$), and case (d) (off resonance with optimum coupling; $\Omega_c = 1.5 \times 10^8$, $\delta - \delta_0 = 1500$).

coupling between the probe beam and the outcoupled atoms at half the optimum strength for complete quantum state transfer, our system acts in a manner analogous to a 50/50 beam splitter, and we find that we can produce entanglement between the amplitude and phase of the outcoupled atoms and the transmitted light when quadrature squeezed light is used to outcouple [7].

We will now show that this procedure allows for a demonstration of the Einstein-Podolsky-Rosen (EPR) paradox [20], which has been shown to be a proof of entanglement [21]. It was first proposed to demonstrate the EPR paradox using optical phase quadratures by Reid [22], followed by an experimental realisation by Ou et al. [23]. To demonstrate entanglement using the EPR paradox, we infer the values of a quadrature on one field via measurements on the corresponding quadrature of the other. Following the EPR proposal, we may do this for conjugate quadratures whose real variances must obey the Heisenberg Uncertainty Principal (HUP). The paradox is demonstrated when the product of the inferred values seemingly violates the minimum set by the HUP. In the present example, by measuring the amplitude and phase quadratures of the optical beam we are able to infer the amplitude and phase quadratures on the atomic beam. Quantitatively, $V_{\rm inf}(\hat{X}^+)V_{\rm inf}(\hat{X}^-) < 1$ is the requirement for demonstrating the EPR paradox, where

$$V_{\rm inf}(\hat{X}^\pm) = V(\hat{X}^\pm) - \frac{[V(\hat{X}^\pm, \hat{Y}^\pm)]^2}{V(\hat{Y}^\pm)}\,, \tag{21}$$

with $V(\hat{X}^\pm, \hat{Y}^\pm) = \langle \hat{X}^\pm \hat{Y}^\pm \rangle - \langle \hat{X}^\pm \rangle \langle \hat{Y}^\pm \rangle$. Here, $\hat{X}^{+(-)}$ refers to the amplitude (phase) quadrature of the atom laser beam, and $\hat{Y}^{+(-)}$ refers to the amplitude (phase) quadrature of the transmitted probe beam, defined by

$$\hat{X}^+ = \int_{x_1}^{x_2} \left(u_\psi^*(x)\hat{\psi}(x) + u_\psi(x)\hat{\psi}^\dagger(x) \right) dx\,, \tag{22}$$

$$\hat{X}^- = i\int_{x_1}^{x_2} \left(u_\psi^*(x)\hat{\psi}(x) - u_\psi(x)\hat{\psi}^\dagger(x) \right) dx\,. \tag{23}$$

$$\hat{Y}^+ = \int_{x_1'}^{x_2'} \left(u_E^*(x)\hat{E}(x) + u_E(x)\hat{E}^\dagger(x) \right) dx\,, \tag{24}$$

$$\hat{Y}^- = i\int_{x_1'}^{x_2'} \left(u_E^*(x)\hat{E}(x) - u_E(x)\hat{E}^\dagger(x) \right) dx\,. \tag{25}$$

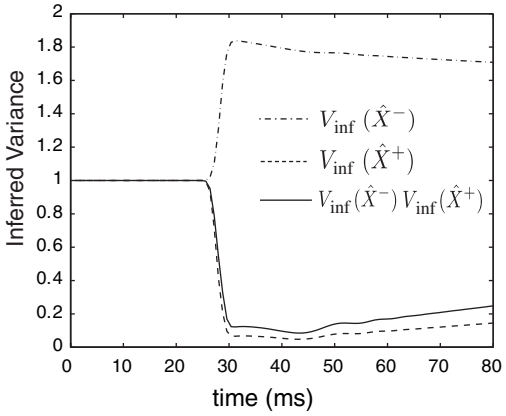

Fig. 4. $V_{\rm inf}(\hat{X}^-)$ (dot-dashed line), $V_{\rm inf}(\hat{X}^+)$, (dashed line), and $V_{\rm inf}(\hat{X}^+)V_{\rm inf}(\hat{X}^-)$ (solid line) for $\Omega_c = 0.75 \times 10^8$ rad s^{-1} and an initial amplitude squeezed optical state with the squeezing parameter $r = 2.0$.

$u_\psi(x,t)$ and $u_E(x,t)$ are arbitrary modes which we choose as plane waves with appropriate wavelengths to match the modes of the outcoupled atoms and transmitted light. We choose x_1 and x_2 to be points in the path of the atom laser beam, and x_1' and x_2' to be downstream of the condensate such that the light operators and atomic operators can be correlated at the same time, i.e. $x_1' = \frac{c}{v_{\rm atom}} x_1$, $x_2' = \frac{c}{v_{\rm atom}} x_2$.

We find that the output atomic beam and the transmitted probe beam are clearly entangled for the appropriate parameters, as shown in Fig. 4, which shows the product of the inferred variances versus time for $\Omega_c = 0.75 \times 10^8\,\mathrm{rad\,s^{-1}}$ and a probe with squeezing parameter $r = 2.0$ [5].

In the case of squeezed light mixed with vacuum on a beamsplitter, for $r = 2.0$, $V_{\rm inf}(\hat{X}^+) = \frac{2e^{-2r}}{1+e^{-2r}} \approx 0.036$, $V_{\rm inf}(\hat{X}^-) = \frac{2e^{2r}}{1+e^{2r}} \approx 1.96$, and $V_{\rm inf}(\hat{X}^+)V_{\rm inf}(\hat{X}^-) = \frac{2}{1+\cosh 2r} \approx 0.071$. These compare quite well to the values which correspond to maximum entanglement in our system $V_{\rm inf}(\hat{X}^+) \approx 0.048$, $V_{\rm inf}(\hat{X}^-) \approx 1.83$, and $V_{\rm inf}(\hat{X}^+)V_{\rm inf}(\hat{X}^-) \approx 0.085$, indicating that our system behaves almost as an ideal beam splitter. We note here that our treatment is idealised, but that we will deal with likely sources of degradation in the following two sections.

5 Homodyne measurements of atomic quadratures

In this section we examine a scheme for transferring quantum information from a propagating atom laser beam to an optical beam, allowing indirect measurement of de Broglie wave quadrature variances via optical homodyning. The strength of this scheme is that it does not require a mode-matched atomic local oscillator, which would be difficult to achieve experimentally. The process involves a reversal of the Raman atom laser output coupling described in the previous sections, so that a two-photon Raman transition now couples the atom beam into a large trapped condensate [10], with highly efficient transfer of the atomic statistics to the optical probe.

The scheme (Fig. 5) consists of a trapped condensate and an incoming atom laser beam of the same species and is essentially a reversal of that described in section 2, with the important difference that stimulation by the trapped condensate now plays an important role. The Hamiltonian and equations of motion are the same apart from different initial conditions, with the atomic beam but not the optical probe beam being occupied at the beginning of the process. To understand the transfer of quantum information in the system we use mode matched quadratures of the probe light and the atomic signal as in section 4.

Figure 6 shows the Raman incoupling dynamics for a continuous, essentially monochromatic atom laser beam. The system consists of a quadrature squeezed atom laser beam in a nearly

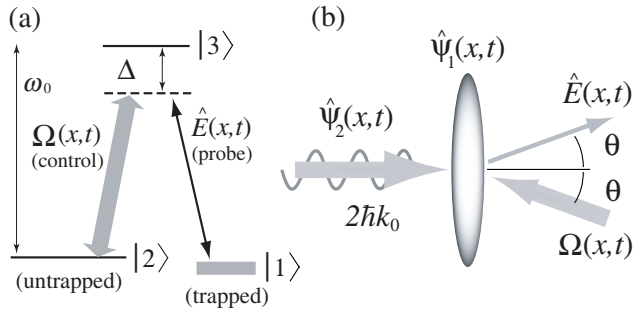

Fig. 5. Raman incoupler. (a) Λ atom. A beam of $|2\rangle$ atoms is coupled to a trapped state $|1\rangle$ via a Raman transition. The two optical fields are a weak probe beam (annihilation operator $\hat{E}(x,t)$), and a classical control beam ($\Omega_{23}(x,t)$). The transition is detuned from the intermediate state by Δ. Wide lines represent highly occupied states. (b) Spatial configuration of the Raman atom laser. Beam atoms ($\hat{\psi}_2(x,t)$) reach the condensate ($\hat{\psi}_1(x,t)$) with momentum $2\hbar k_0$, which is transferred during incoupling by absorption and emission of a light quanta at angle θ and momenta $\mp\hbar k_0$ with respect to the propagation axis.

monochromatic state (wavevector $2k_0$) which enters from the left. The atoms are incoupled via the reversed Raman scheme, emitting probe photons. Once the front of the beam crosses the interaction region the system is approximately in a steady state (except for the gradual transfer of atoms into the trapped condensate), with a constant probe output. We see that the quadrature variances of the emitted probe light reach steady state values very close to the atom laser variances.

As quantum states are very fragile we must consider possible sources of loss. Apart from the stability of the lasers used, the main sources of possible signal degradation are spontaneous emission losses and collisional phase noise. The effect of spontaneous emission can be estimated from the spontaneous emission rate for a transition with energy $\omega_0 = k_0 c$ radiating into a continuum, $\gamma_{\rm sp} = k_0^3 |d_{13}|^2/3\pi\hbar\epsilon_0$. The spontaneous loss during the incoupling is then $L_{\rm sp} = \gamma_{\rm sp} \int dx \int dt\ \langle \hat{\psi}_3^\dagger(x,t)\hat{\psi}_3(x,t)\rangle$. Using the adiabatically eliminated expression for the excited state $\langle \hat{\psi}_3^\dagger(x,t)\hat{\psi}_3(x,t)\rangle \approx \langle \hat{\psi}_2^\dagger(x,t)\hat{\psi}_2(x,t)\rangle(\Omega_{23}/\Delta)^2$, and the fact that each excited atom on average remains excited for time $T_{\rm Rabi}/4$, we have approximately $L_{\rm sp} \leq \gamma_{\rm sp}\bar{N}_3 T_{\rm Rabi}/4$, where $\bar{N}_3$ is the total number of excited atoms transferred per squeezed mode. For the incoupling process to remain coherent, we require $L_{\rm sp}/\bar{N}_3 \ll 1$, and for our parameters we find $L_{\rm sp}/\bar{N}_3 \approx 0.04$. We can now estimate the effect on the signal using a beam splitter which mixes the signal and vacuum with reflectivity η ($\approx$0.04 here). The probe variances then become $V(\hat{X}_E^\pm) = (1-\eta)V(\hat{X}_\psi^\pm) + \eta$, acceptable for small η. The collisions between the beam and condensate atoms will have two undesired effects. Firstly, there will be a mean-field shift to the condensate energy which will rotate the quadrature phases. This will be negligible when the number of incoupled atoms is much smaller than the condensate occupation, which will be the case in any practical realisation of the scheme. The second effect will be that of phase-diffusion of the beam, which to a first approximation will cause an increase in the variance of the phase quadrature. We may consider this effect by noting that the velocity transferred to ^{23}Na by the Raman transition can be up to 6 cm/s (1.2 cm/s for ^{87}Rb). Using a single-mode expression for the phase diffusion [24] and the parameters of Fig. 6, we find that ^{23}Na can travel up to 3 mm and ^{87}Rb up to 600 μm in their respective coherence times. As this is larger than the diameter of present condensates, the effect will be small. Another issue which will arise is that the probe beam will be emitted into a narrow cone rather than as a well collimated beam. This can be simply overcome using linear optical elements. An important consideration is the role of condensate phase in our scheme. Although for simplicity we have treated the BEC as a coherent state, in practice this does not pose a significant restriction. A reasonable model for a BEC is a coherent state with an a priori random phase. It is clear from that the dynamics are sensitive to the phase of $\phi_1(x)$. However, from our numerical simulations we have found

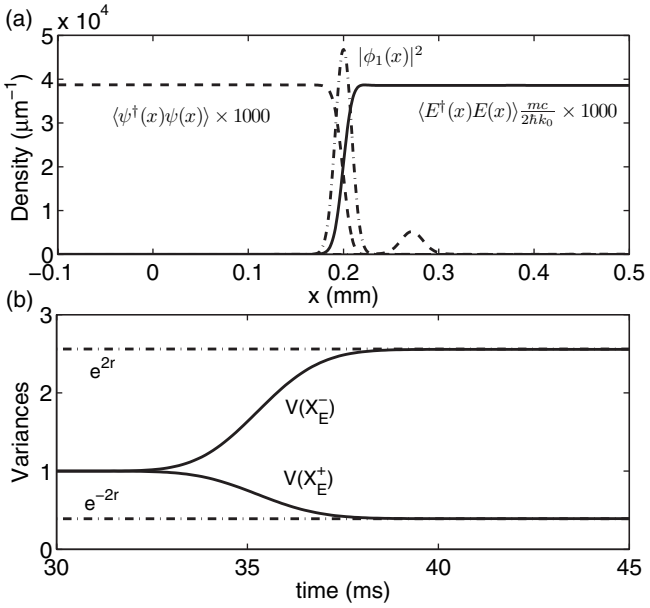

Fig. 6. Incoupling a continuous atom laser beam. (a) A snapshot of the atomic beam (dashed line), condensate (chain line) and probe (solid line) during incoupling. The small blip of atoms on the right is a transient effect. (b) The development of the optical quadratures (solid lines) as the front of the atom laser beam crosses the interaction region. The zero of the time axis is arbitrary. The chain lines show the variances of the 4 dB squeezed atomic beam.

that changing the initial phase of the condensate simply rotates the phase space quadratures of the output optical field, so that on an experimental run the spontaneously chosen phase will be automatically compensated for when all angles are scanned over during optical homodyne detection. Finally, we address the effect of a thermal component on the phase stability of the condensate during incoupling. Since phase diffusion is most significant at high temperatures we use quantum kinetic theory [25]. We find that during the incoupling interaction time the phase diffusion is entirely negligible for our parameters and a temperature of order $\sim$100 nK. The decay of the relevant two-time correlation function, $\langle \phi_1^\dagger(x,t)\phi_1(x',t')\rangle$, is typically at the level of one part in 10^8 during the incoupling time.

6 Teleportation without shared entanglement

The instantaneous, disembodied transport of matter through space is of course, absolutely forbidden by the laws of nature. However, in 1993, a proposal by Bennett et al. [26] used the term *teleporting* to describe a scheme which uses quantum entanglement to transfer an unknown discrete variable quantum state between a sender and a receiver. The protocols of this scheme were later extended to continuous variable (CV) transfer [27,28], and have been demonstrated experimentally, with fidelities of up to 0.85 ± 0.05 for the transfer of an unknown CV quantum state [29]. In this section we propose a scheme which allows an atom laser beam to disappear at one location and reappear at another, without the use of shared entanglement between the sender and receiver. We will go beyond information available from intensity measurements and determine the quantum efficiency of state transfer. Although our scheme is quite distinct from what is normally termed quantum teleportation, we feel that it is closer in spirit to the original fictional concept and so use this term. What differentiates our scheme from what is usually termed quantum teleportation is that we do not require the sender and receiver to share entangled states. We avoid this requirement as there is no measurement step involved in sending the information. As we do not require the generation and distribution of entangled states it may be possible to achieve a much higher teleportation fidelity than with traditional quantum teleportation.

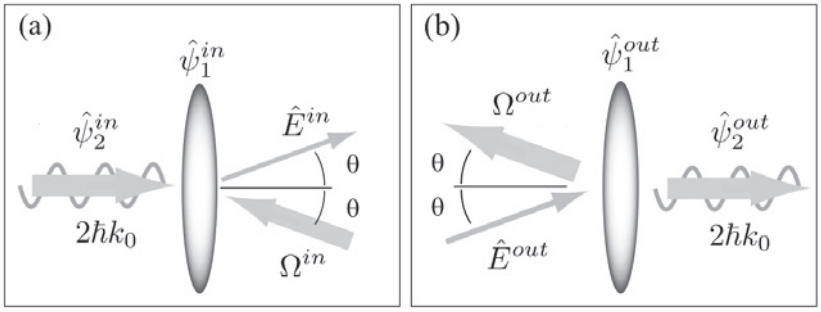

Fig. 7. The sending, $\hat{\psi}_1^{in}$, and receiving, $\hat{\psi}_1^{out}$, stations for the teleporter. (a) the *sender*, which absorbs the propagating atoms and transmits the optical signal containing the quantum information. (b) the *receiver* which absorbs the optical signal and uses the information contained in it to reproduce the original atomic pulse. Ω^{in} and Ω^{out} are the classical control fields, while $\hat{E}^{in}$ and $\hat{E}^{out}$ are the same probe field, created by the incoupling and absorbed by the outcoupling process.

Our system is shown schematically in Fig. 7. As can be seen, this is the Raman incoupler used to allow for indirect quadrature measurements on an atom laser beam, coupled via the optical probe field to a Raman outcoupler which transfers the quantum statistics of the probe to the subsequent atom laser beam. The sending stage of the scheme is shown in Fig. 7(a), where the input atom laser beam ($\hat{\psi}_2^{in}$) is coupled into the condensate ($\hat{\psi}_1^{in}$). The quantum information held in the beam is transferred to the probe field ($\hat{E}^{in}$). The internal Raman energy level configuration allows for stimulated transitions between the trapped and untrapped fields. These transitions are stimulated by both intense optical fields (control), denoted by the Rabi frequencies $\Omega^{in/out}(x,t)$, and highly occupied trapped bosonic matter fields ($\hat{\psi}_1^{in/out}$). The optical probe propagates some distance between the two condensates, and is used ($\hat{E}^{out}$) to outcouple the atom laser field from the second condensate ($\hat{\psi}_2^{out}$). The preparation of the sending and receiving condensates and the control lasers needs only the passing of classical information, and can be done without knowing the quantum state of the input beam. State transfer from the input atom laser pulse to the probe field happens automatically given the appropriate conditions, as shown by Bradley et al. [8]. At the receiver, the state of the probe field is transferred to the output atomic pulse [6]. If the required conditions are met, there will be a complete transfer of the quantum information contained in the first pulse, via the probe field, to the second. We note that technically our scheme would realise a very efficient quantum channel [30,31] to transfer information between condensates.

We analyse the system using the one-dimensional model and computational technique of section 2. Results from our one-dimensional numerical calculations are shown in Fig. 8. The input atomic pulse has $n_0 = 5 \times 10^3$, with momentum wavevector $2k_0$, coupled into the initial condensate, where $k_0 = 8 \times 10^6\,\mathrm{m}^{-1}$, giving an atom laser beam velocity of $v_{\mathrm{atom}} = 1.1\,\mathrm{cm\,s}^{-1}$. We use $N_0 = 10^6$ atoms at each site, trapped with potentials $V(x) = m\omega_t^2 x^2/2$ and frequencies $\omega_t = 5\,\mathrm{Hz}$. In all cases we operate at the optimal efficiency point for the signal so that the ratio of the condensate width to the mean beam velocity is tuned to one quarter of a Rabi cycle, $T_{\mathrm{Rabi}} \approx 4\sqrt{\hbar/m\omega_t}(m/2\hbar k_0)$. The two condensates are shown by the dashed lines, which are given as 1 mm apart, merely for convenience. In the top panel, an atom laser pulse is about to enter the first condensate. The middle two panels show the pulse being incoupled and the probe field, initially vacuum in this example, transmitting between the two condensates. The beginnings of the pulse can be seen as the outcoupling process proceeds. In the lowest panel, the outcoupling process has been completed and a replica of the initial pulse is propagating away from the second condensate. Apart from the information needed to prepare the two condensates with near identical numbers and the control fields with similar intensities, no information except that contained in the propagating probe field has been exchanged. In principle, this scheme can be operated with a very high fidelity, as long as the appropriate Rabi frequencies are matched at each site. Once this is achieved, the remaining sources of degradation are phase diffusion from

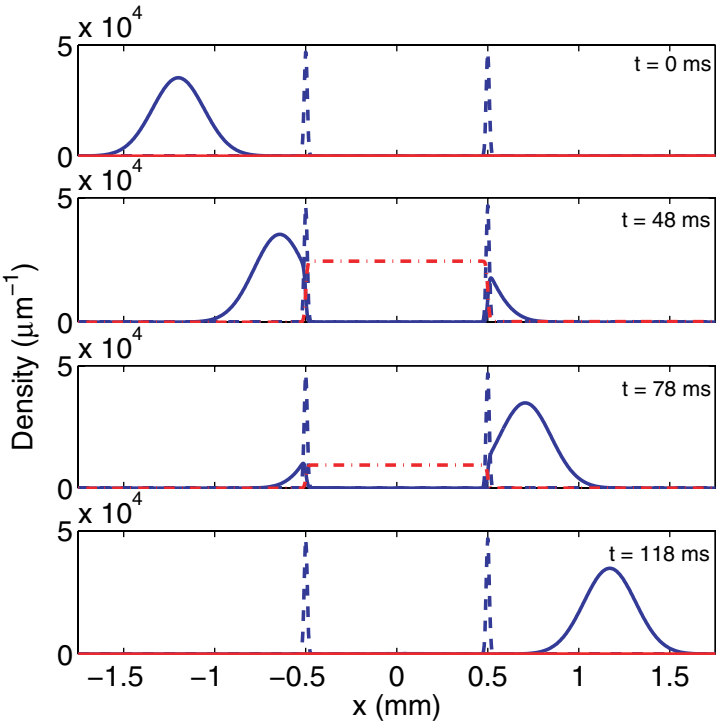

Fig. 8. At the top, the initial atomic pulse (solid curve) is shown about to enter the sending condensate (left dashed curve). The second and third pictures show the pulse partially absorbed, with an output pulse exiting the receiving condensate (right dashed curve). In the bottom picture, the process is completed, with a reconstructed atom laser pulse propagating in free space. The atom pulse and optical probe (dashed-dotted curve) are magnified by factors of 1000 and $1000 \times mc/2\hbar k_0$ to plot them on the condensate scale.

collisional interactions and spontaneous emission from the excited electronic levels of the two trapped condensates. As shown in the previous section, these can be minimised and would need to be significant before the efficiency of the process fell to the 2.2% obtained in the Ginsberg experiment [32].

7 Conclusions

In conclusion, we have shown that the development of the Raman atom laser has opened up a whole new field of possibilities for the coherent manipulation of matter waves and the transferring of quantum information between bosonic atoms and light. We have shown that sources of degradation of this transfer can be minimised by careful control of experimental parameters. The Raman outcoupling and incoupling techniques described here need no new technologies and can be realised in existing laboratories. A possible strong advantage of these Raman schemes over schemes depending on EIT is that they do not operate at resonance, where spontaneous emission can become a real problem.

This work was supported by the Australian Research Council and the Queensland state government.

References

1. G. Lenz, P. Meystre, E.M. Wright, Phys. Rev. Lett. **71**, 3271 (1993)
2. S.L. Rolston, W.D. Phillips, Nature **416**, 219 (2002)
3. P.L. Knight, Science **310**, 631 (2005)

4. G.M. Moy, J.J. Hope, C.M. Savage, Phys. Rev. A **55**, 3631 (1997)
5. H.A. Bachor, T.C. Ralph, *A Guide to Experiments in Quantum Optics* (Wiley-VCH, Weinheim, 2004)
6. S.A. Haine, J.J. Hope, Las. Phys. Lett. **2**, 597 (2005)
7. S.A. Haine, M.K. Olsen, J.J. Hope, Phys. Rev. Lett. **96**, 133601 (2006)
8. A.S. Bradley, M.K. Olsen, S.A. Haine, J.J. Hope, Phys. Rev. A **76**, 033603 (2007)
9. M.K. Olsen, A.S. Bradley, S.A. Haine, J.J. Hope, Nucl. Phys. A **790**, 733c (2007)
10. V.V. Paranjape, P.V. Panat, S.V. Lawande, Int. J. Mod. Phys. B **17**, 4465 (2003)
11. A.S. Bradley, M.K. Olsen, S.A. Haine, J.J. Hope (2007) (preprint) [arXiv:0706.0062]
12. K.V. Kheruntsyan, M.K. Olsen, P.D. Drummond, Phys. Rev. Lett. **95**, 150405 (2005)
13. L.M. Duan, A. Sørensen, J.I. Cirac, P. Zoller, Phys. Rev. Lett. **85**, 3991 (2000)
14. H. Pu, P. Meystre, Phys. Rev. Lett. **85**, 3987 (2000)
15. S.A. Haine, J.J. Hope, Phys. Rev. A **72**, 033601 (2005)
16. H. Jing, J.-L. Chen, M.-L. Ge, Phys. Rev. A **63**, 015601 (2000)
17. M. Fleischhauer, S. Gong, Phys. Rev. Lett. **88**, 070404 (2002)
18. E. Tiesinga, A.J. Moerdijk, B.J. Verhaar, H.T.C. Stoof, Phys. Rev. A **46**, 1167(R) (1992)
19. W.P. Bowen, P.K. Lam, T.C. Ralph, J. Mod. Opt. **50**, 801 (2003)
20. A. Einstein, B. Podolsky, N. Rosen, Phys. Rev. **47**, 777 (1935)
21. M.J. Mallon, M.D. Reid, M.K. Olsen, J. Phys. B **41**, 015501 (2008)
22. M.D. Reid, Phys. Rev. A **40**, 913 (1989)
23. Z.Y. Ou, S.F. Pereira, H.J. Kimble, K.C. Peng, Phys. Rev. Lett. **68**, 3663 (1992)
24. M.J. Steel et al., Phys. Rev. A **58**, 4824 (1998)
25. C.W. Gardiner, P. Zoller, Phys. Rev. A **58**, 536 (1998)
26. C.H. Bennett et al., Phys. Rev. Lett. **70** (1993)
27. L. Vaidman, Phys. Rev. A **49**, 1473 (1994)
28. S.L. Braunstein, H.J. Kimble, Phys. Rev. Lett. **80**, 869 (1998)
29. N. Takei et al., Phys. Rev. A **72**, 042304 (2005)
30. Y.-J. Gu, C.-M. Yao, Z.-W. Zhou, G.-C. Guo, J. Phys. A **37**, 2447 (2004)
31. C.H. Bennett, P.W. Shor, Science **303**, 1784 (2004)
32. N.S. Ginsberg, S.R. Garner, L.V. Hau, Nature **445**, 623 (2007)